ELSEVIER

Journal of Alloys and Compounds 275–277 (1998) 759–764

Journal of ALLOYS AND COMPOUNDS

Gas-phase reactions of laser-ablated f element ions with cyclic hydrocarbons: examining ion ablation and reaction mechanisms

John K. Gibson

Chemical and Analytical Sciences Division, Oak Ridge National Laboratory, P.O. Box 2008, Oak Ridge, TN 37831-6375, USA

Abstract

Time-of-flight mass spectrometry is employed to study reactions such as: $Ln^+ + c\text{-}C_6H_{10} \rightarrow Ln^+ - C_6H_6 + 2H_2$. Discrepant reactivities of various Ln^+ parallel the energy needed to excite the Ln^+ to a divalent electronic configuration. Metal ions produced by laser ablation may possess substantial kinetic and internal energies which can alter reactivities; we report here on experiments which illuminate formation and reactions of ablated Ln^+. Effects of target composition on reactivities of a particular lanthanide were studied for compounds ablated sequentially, or simultaneously employing isotopically enriched $^{A}Ln_2O_3$. Differing reactivities of Ho^+ from three compounds, and of Nd^+ from $^{142}Nd_2O_3$ and Nd_2Te_3 may indicate a role of excited Ln^+*. Yields of Ln^+ (Ln=Nd or Gd) simultaneously ablated from LnB_6 and $^{A}Ln_2O_3$ were widely disparate, with most Ln^+ derived from the oxide, suggesting electron transfer processes such as $Ln^* + O^* \rightarrow Ln^+ + O^-$. Speciation in the initial stage of ablation, prior to isotopic mixing, was indicated by the predominance of $^{142}NdO^+$ from $^{142}Nd_2O_3$–Nd_2Te_3. The reaction, Ln^++benzene, was studied with deuterated benzenes. Benzyne complexes from benzene-1,3,5-d_3 were *d*-enriched, reflecting the kinetic isotope effect (KIE); also, H_2-loss indicated elimination from non-adjacent sites or H–D scrambling. Comparative condensation and dehydrogenation yields from C_6H_6 and C_6D_6 are explained by energy dissipation into vibrational modes which favors Ln^+–C_6D_6, and the KIE which favors Ln^+–C_6H_4. © 1998 Published by Elsevier Science S.A.

Keywords: Time-of-flight mass spectrometry; Ln^+; Laser ablation; Target composition

1. Introduction

We reported previously on the relative dehydrogenation activities of lanthanide ions, Ln^+, determined from the following type of gas-phase reaction with cyclic hydrocarbons [1]:

$$Ln^+ + \text{cyclo} - C_6H_{6+2m} \rightarrow Ln^+ - C_6H_{6+2m-2e} + eH_2 \quad (1)$$

2

For $e \geq 1$ discrepant reactivities across the lanthanide series paralleled the energies to promote the ground-state Ln^+ to an electronic configuration with two *non-f* (i.e. 5d/6s) electrons suitable for oxidative insertion into a C–H bond. Recent results for resonant laser ablation spectroscopy of lanthanides [2] suggested formation of substantial excited-state ablated Ln^+*, advising consideration of the role of excited-state ions in the chemistry of ablated Ln^+. The correspondence between our Ln^+ reactivity results and those from FTICR-MS [3] is remarkable in view of the discrepant conditions; the FTICR experiments employed thermalized (ground-state) Ln^+, whereas we reacted energetic laser-ablated ions within $\sim 10^{-5}$ s of formation. Ion kinetic energy (KE) can enable endothermic dehydrogenation processes [4,5], although in the present experiments any KE effect was constant; however, discrepant populations of electronically excited Ln^+* might obscure ground-state chemistries. Excited M^+* chemical effects have been demonstrated for several d-block transition metals [6] as well as Yb^+* [7]. The initial results for reactions of nascent laser-ablated Ln^+ confirmed the phenomenological validity of this approach in distinguishing intrinsic Ln^+ chemistry, but did not fully elucidate the origin of the distinctions, specifically the role of Ln^+* [1]. Though the Ln^+ KEs did not affect *comparative* reactivities it is of interest to assess the effect of collisional energy on mechanistics to ascertain if a (low-energy) α,β-hydrogen elimination model is applicable and how excited complex ions avoid fragmentation.

The experiments reported here probe formation and reactivities of Ln^+ ablated from disparate solids; the results elucidate the role of Ln^+*. Studies with isotopically labeled Ln compounds illuminate the laser ablation process and formation of molecular ions. Reactions of laser-ablated

0925-8388/98/$19.00
PII: S0925-8388(98)00435-6

Ln^+ with deuterated benzenes probed dehydrogenation mechanistics and energy dissipation in gaseous organometallic complexes.

2. Experimental

The general approach is similar to the laser ablation molecular beam (LAMB) method described by Sato and co-workers [8]. The experimental configuration and general techniques have been described [1,9] and only key features are included here. A pulsed XeCl excimer laser ($\lambda = 308$ nm) was focused to a ~0.5-mm^2 spot, approximately normal to a target surface. The irradiance was adjusted within a range of about a decade to provide optimal M^+ intensity; a typical pulse energy on the target was ~1 mJ which implies an energy density of ~200 mJ cm^{-2} and a nominal irradiance of ~10^7 W cm^{-2} assuming a pulse duration of ~15 ns.

A constant pressure of reactant gas, undetermined but estimated to be of the order of ~0.1 Pa, was established in the trajectory of ablated ions ~1 cm from the target. Unreacted and product ions were determined by injecting a portion (~6-mm diameter transverse cylinder) of the propagating ablation plume into a reflectron time-of-flight mass spectrometer. Ion sampling occurred ~3 cm from the target and the delay, t_d, between the laser pulse and the ion injection pulse could be varied—ion signals were typically measurable for t_d in the range of 10–100 μs. Optimal product detection was obtained for $t_d \approx 35$ μs and most of the results here employed this value which corresponds to an ion velocity of $\{3\ cm/35\ \mu s\} \approx 10^3$ m s^{-1}. For a M^+ of mass 200 Da this represents a KE of ~1 eV or 100 kJ mol^{-1}; all examined Ln^+ had similar velocity, mass and KE.

Three types of target were prepared from materials of ≥99.9% purity (except 99.5% LnB_6). Unless an enriched isotope is specified ('^{A}Ln') the lanthanides were in their naturally occurring isotopic abundances. Pieces of $CeSi_2$(s) and Ho° (metal) were used as supplied. The Tb^+ sources were $Tb_{50}Ho_{50}$ and Tb-contaminated '$Nb_{48}Ta_{52}$' arc-melted alloys [1]. The other targets were prepared by mixing powders of lanthanide compound(s) and copper and forming into 3-mm diameter pellets. The copper matrix targets had the following aggregate molar compositions: (A) 4.2% HoF_3/96% Cu; (B) 2.3% $HoTe_{3/2}$/98% Cu; (C) 2.2% $^{142}NdO_{3/2}$/2.0% $NdTe_{3/2}$/96% Cu; (D) 2.9% $^{142}NdO_{3/2}$/4.3% NdB_6/93% Cu; (E) 3.5% $^{160}GdO_{3/2}$/6.3% GdB_6/90% Cu. The enriched $^A Ln_2O_3$(s) (ORNL Isotopes Dept.) had the following isotopic compositions:

$^{142}Nd_2O_3$	98.3% ^{142}Nd/0.7% ^{143}Nd/0.6% ^{144}Nd/≤0.2% other ^{A}Nd
$^{160}Gd_2O_3$	98.1% ^{160}Gd/0.9% ^{158}Gd/0.4% ^{157}Gd/0.3% ^{156}Gd/<0.2% other ^{A}Gd

The lanthanide oxides were (fine) powders of indeterminate particle size; target homogeneity on the scale of the ~0.5-mm^2 laser spot was confirmed by establishing consistent results for several target locations—only minor variations in ion yields could be discerned. Simultaneous ablation of $^{142}Nd^+$ and normal Nd^+ from the $^{142}Nd_2O_3$–Nd_2Te_3–Cu target confirmed homogeneity.

The organic reagents were commercial products, handled as described previously [1]. The specifications were as follows: benzene and benzene-d_6, 99.9%; benzene-1,3,5-d_3 ($C_6H_3D_3$), 98%; 1,5-cyclooctadiene (COD), 99%; 1-methyl-1,4-cyclohexadiene (Me-C_6H_7), 99%; and perfluorophenanthrene ($C_{14}F_{24}$), mass spectrometer calibrant.

3. Results and discussion

3.1. Ablation of Ln^+ from disparate solids

3.1.1. Ho^+-sequential ablation

The three Ho targets, Ho°, HoF_3–Cu and Ho_2Te_3–Cu, were mounted together on a planchet which could be translated in situ to determine comparative reactivities of Ho^+ ablated under comparable conditions; it was necessary to vary the irradiance by up to an order of magnitude to achieve practical Ho^+ yields (applied irradiances decreased as: $Ho_2Te_3 \geq HoF_3 > Ho°$). A typical mass spectrum for the reaction of Ho^+ from these three targets with COD is shown in Fig. 1; intensities of Ho^+ decreased as $Ho_2Te_3 > Ho° \geq HoF_3$, while the intensities of the main product, Ho^+–COT (COT = cyclooctatetraene, C_8H_8), de-

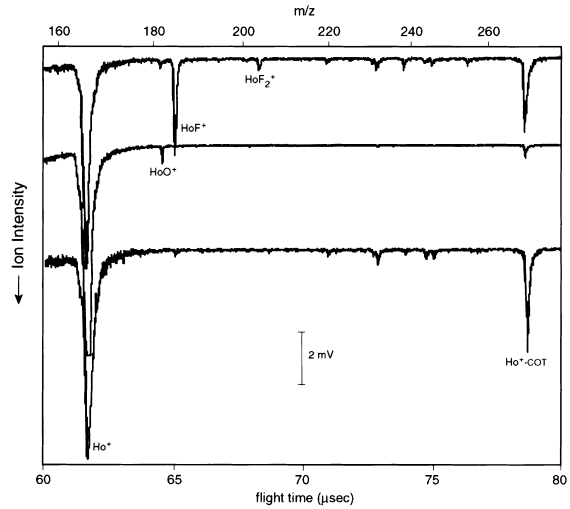

Fig. 1. Mass spectra for Ho^+ + 1,5-cyclooctadiene. The spectra are for Ho^+ from three targets: top, HoF_3–Cu; middle, Ho_2Te_3–Cu; bottom, Ho°.

creased as $Ho^{\circ} \geq HoF_3 > Ho_2Te_3$. For the dehydrogenation of $Me–C_6H_7$ to yield Ho^+–toluene, the relative intensities of bare Ho^+ decreased as $Ho^{\circ} > Ho_2Te_3 > HoF_3$, while the product ion yields decreased as $HoF_3 > Ho^{\circ} > Ho_2Te_3$. The principal observation was of diminished reactivity of Ho^+ ablated from Ho_2Te_3.

3.1.2. Isotopically enriched Nd^+ and Gd^+-simultaneous ablation

Lanthanides ablated from disparate compounds under identical conditions were studied using the mixtures, $^{142}Nd_2O_3–Nd_2Te_3–Cu$, $^{142}Nd_2O_3–NdB_6–Cu$ and $^{160}Gd_2O_3–GdB_6–Cu$. The latter two targets gave similar results, exemplified in Fig. 2 for $^{142}Nd_2O_3–NdB_6–Cu$. The oxide-derived ions, $^{142}Nd^+$ and $^{160}Gd^+$, were dominant for all target spots and values of t_d, even after several thousand laser shots by which point steady-state material loss should prevail—Ln^+ from LnB_6 was minor. Injection of $C_{14}F_{24}$ (Fig. 2, bottom) produced LnF^+ and LnF_2^+ [10] and concurrently an enhancement in Ln^+ from LnB_6, which can be attributed to: $Ln^* + C_{14}F_{24} \rightarrow Ln^+ + C_{14}F_{24}^-$. The typical results for $^{142}Nd_2O_3–Nd_2Te_3–Cu$ shown in Fig. 3 reveal substantial Nd^+ from both compounds. Dehydrogenation products of the reaction of Nd^+ with COD are shown in the bottom of Fig. 3; the peak assignments are consistent with other results where Nd^+–COT was the dominant product with minuscule Nd^+–C_8H_{10}, and no Nd^+–COD. The $^{142}Nd^+$–COT yield was diminished relative to that of bare $^{142}Nd^+$, suggesting that Nd^+ from Nd_2Te_3 was more reactive than Nd^+ from Nd_2O_3. Both the Ho^+ and Nd^+ results indicate precursor-dependent reactivities. It is also noted that the $^{142}Nd_2O_3–Nd_2Te_3–Cu$ spectrum in Fig. 3 (top) indicates that the

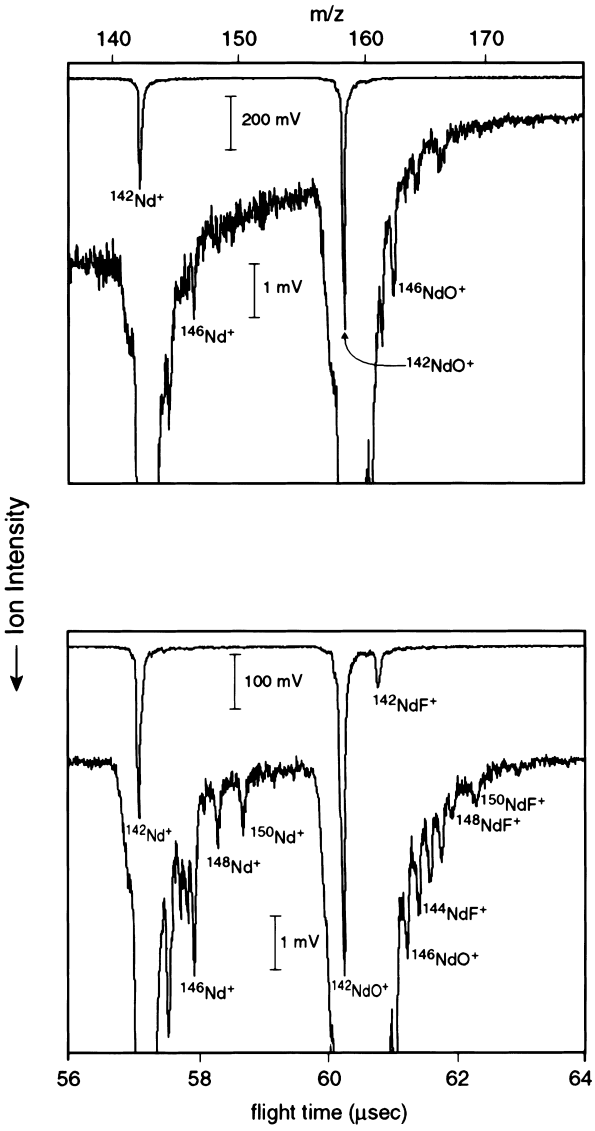

Fig. 2. Mass spectra for the $^{142}Nd_2O_3–NdB_6–Cu$ target. Top, ablation into vacuum; bottom, ablation into $C_{14}F_{24}$(g).

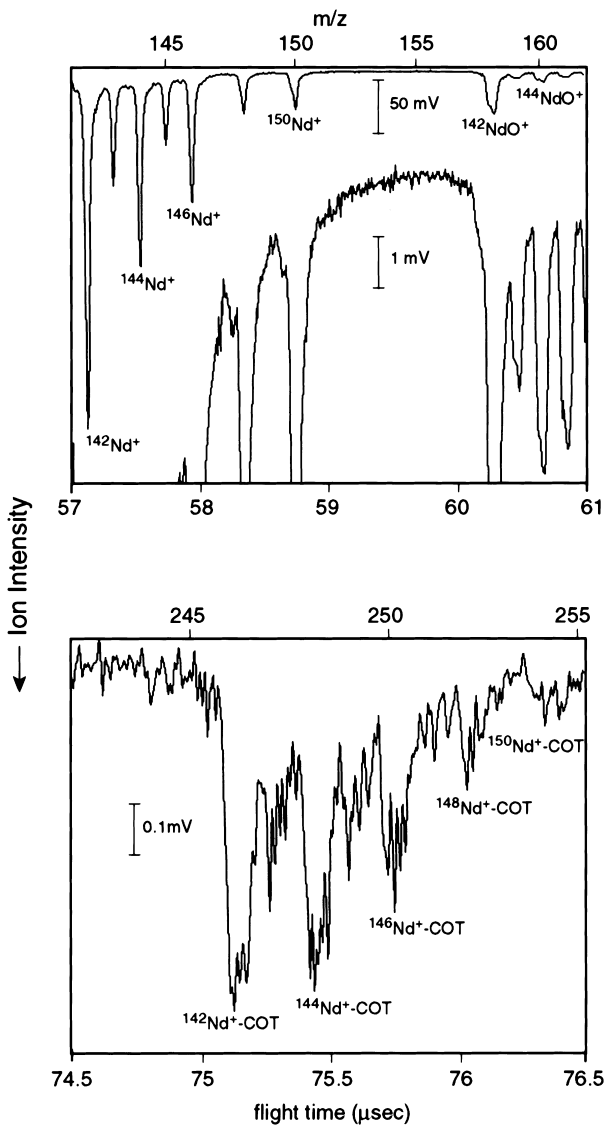

Fig. 3. Mass spectrum for reaction of Nd^+ from $^{142}Nd_2O_3–Nd_2Te_3–Cu$ with 1,5-cyclooctadiene.

dominant oxide ion, $^{142}NdO^+$, derived directly from the solid oxide.

3.1.3. Analysis of precursor effects

The results for ablation of lanthanides from disparate solids illuminates the ablation process as well as reactivities of ablated Ln^+. Studies of laser ablation mechanisms have addressed target–laser interactions and formation of polyatomic species [11]. Cluster formation has been attributed to both gas-phase recombination [12] and direct ejection [13]; an investigation of lanthanide oxide cluster formation indicated coalescence of smaller species [14]. The prevalence of $^{142}NdO^+$ from $^{142}Nd_2O_3$–Nd_2Te_3–Cu indicates formation of LnO^+ prior to atomistic mixing, either by direct ejection from the solid or prompt atomic recombination. Despite the formation of molecular ions at/near the solid surface, studies have shown that the speciation of ablated ions does not generally reveal the chemical nature of the precursor solid [15].

Discrepant Ln^+ yields from oxide and boride solids suggests chemi-ionization effects prior to atomistic mixing. The greater Ln^+ yield from the oxide is consistent with enhanced ionization by electron transfer processes such as $Ln^* + O \rightarrow Ln^+ + O^-$; the electron affinity (EA) of O (1.46 eV) exceeds that of B (0.28 eV) [16]. Some Ln^+ could also derive from dissociative processes such as $LnO^* \rightarrow Ln^+ + O^-$. The slightly greater yield of Nd^+ from Nd_2Te_3 compared with Nd_2O_3 is consistent with EA[Te]=1.97 eV [16]. The precursor-dependent differences in Ln^+ yields indicate prompt ionization near the target surface in accord with resonant laser ablation evidence for quasi-thermal ionization within <100 ns of ablation [2].

Previously determined reactivities of nascent laser-ablated Ln^+ suggested primarily ground (or low-lying) electron configurations for ablated Ln^+ which resulted in clear distinctions between different Ln [1]. The distinctive behaviors could be attributed to discrepant reactivities of the dominant ground-state Ln^+ and/or to disparate, albeit minor, populations of excited Ln^+*—both effects would parallel the energy to promote ground Ln^+ to a divalent state with two non-f valence electrons. The present results suggest disparate reactivities for the same Ln^+ ablated from different compounds; a reasonable explanation is precursor-dependent abundances of Ln^+* which are more effective at C–H activation. Although the lifetimes of many Ln^+* are too short (<1 μs) to manifest in LAMB studies, long-lived states are known (e.g. >7 day $^2F_{7/2}Yb^+$*) [17] and several low-lying (<1 eV) Ln^+* may be long-lived compared to the ~10-μs LAMB timeframe. Full excitation to a divalent configuration would not be necessary to facilitate C–H activation via a 'curve-crossing' mechanism such as postulated by Schwarz and co-workers [3]. The present results do not diminish the value LAMB approaches for elucidating f-element ion-molecule reactions, but do advise careful interpretation of observed reactivities; although it is possible that Ln^+* are important, the discrepant energies necessary to achieve a reactive divalent configuration remain distinctly manifested. The observed precursor effects recommend comparing reactivities for M^+ simultaneously ablated from chemically similar environments in a multi-component target. As it has been reported that substantial M^+* populations may persist after $>10^5$ quenching collisions [18] the role of Ln^+* must be addressed in longer time-scale multi-collision experiments such as with FTICR [19].

3.2. Reactions of Ln^+ with deuterated benzenes

3.2.1. Benzene-1,3,5-d_3 ($C_6H_3D_3$)

To ascertain the validity of a dehydrogenation mechanism of oxidative insertion of Ln^+ into a C–H bond followed by β-H elimination, Ln^+ were reacted with benzene-1,3,5-d_3 for which this model predicts exclusively HD-loss. The yields of Ln^+–benzyne, were typically small (<0.1%), precluding quantitative assessment of H_2-, HD-, and D_2-loss. For Tb^+–benzyne, the approximate yields were: ~70% HD-loss; <20% D_2-loss; and ~25% H_2-loss. The greater Ce^+–benzyne yields provided the following: ~60% HD-loss; ~10% D_2-loss; and ~30% H_2-loss. Statistically random elimination would result in 60% HD-loss and 20% each of D_2- and H_2-loss. While D_2-loss was below the statistical value, H_2-loss was enhanced, consistent with the KIE. The apparent non-preference for α,β-elimination may reflect post-collision hydrogen scrambling of the benzene-1,3,5-d_3 since the Ln^+–benzene collision energy of ~30 kJ mol^{-1} corresponds to a temperature of ~4000 K.

Ortho-, *meta*-, and *para*-benzyne result from 1,2-(α,β-), 1,3-, and 1,4-H_2 elimination from benzene, respectively, and the comparative thermodynamics of these elimination processes can be assessed. Although *m*-benzyne (i.e. H_2- or D_2-loss from benzene-1,3,5-d_3) has been isolated [20] and is ~40 kJ mol^{-1} less stable than *o*-benzyne [21], the value of EA[*m*-benzyne] is ~30 kJ mol^{-1} greater than that of EA[*o*-benzyne] [22], and the isomer stabilities might be comparable in a Ln^+-benzyne complex due to electron donation from the metal center to the ligand. It is notable that a reaction considered above, $Ho^+ + Me–C_6H_7 \rightarrow Ho^+$–toluene$+H_2$, *formally* proceeds by 1,4-H_2 elimination.

3.2.2. Mixed protonated and deuterated benzene

As reported previously for Ln^++benzene reactions [1] condensation became increasingly significant relative to (endothermic) dehydrogenation as the ion KE decreased. It is presumed that lower collision energies stabilize condensation adducts from fragmentation. Condensation should similarly be enhanced by providing additional energy dissipation channels in the nascent complex such as by increasing the vibrational density of states by D-substitution; this has been demonstrated for Al^+–C_6D_6 [23]. Selected Ln^+ were reacted with a mixture of C_6H_6 and

C_6D_6 at approximately equal partial pressures (confirmed by in situ EI-MS). Typically, Ce^+ was the most reactive Ln^+ and, accordingly, provided the most complete results, such as shown in Fig. 4 (the complex ion yields were $<1\%$ of the Ce^+ intensity); the following yield relationships were derived: $\{Ce^+–C_6H_4\}/\{Ce^+–C_6H_6\}=2.1\pm0.3$ and $\{Ce^+–C_6D_4\}/\{Ce^+–C_6D_6\}=1.4\pm0.2$. The results are consistent with both enhanced stabilization of nascent $Ce^+–C_6D_6$ and a greater dehydrogenation rate for C_6H_6 in accord with the KIE. These effects were also qualitatively indicated for $Tb^+ + C_6H_6/C_6D_6$.

The present results can be compared with models [24] and experiments [23] involving associative reactions and deuteration effects. The present conditions carry out reactions within ~30 μs of Ln^+ formation and detect products within 100 μs. Considering the reaction pathlength and estimated local pressure (of the order of ~0.1 Pa), a Ln^+ should typically experience perhaps a few collisions prior to detection; in accord with primarily bimolecular processes, the dependence of complex ion yields on reactant pressure was approximately first-order [1]. In contrast, FTICR experiments track reactions for $\gtrsim 1$ s and many collisions may occur [17]—processes such as complex ion dissociation and radiative cooling can be studied there [24]. Roughly, radiative cooling of M^+–benzene complexes occurs on a timescale of ~100 ms and unimolecular dissociation on a timescale of 100 μs [24]—it is probable that many of the complex ions detected under the present conditions ($\lesssim 100$ μs) are ultimately unstable to dissociation; Ln^+ from metastable decay of complex ions in the flight tube were not discernible under the present experimental conditions. Even if transient, the studied complexes coherently elucidate metal ion chemistry.

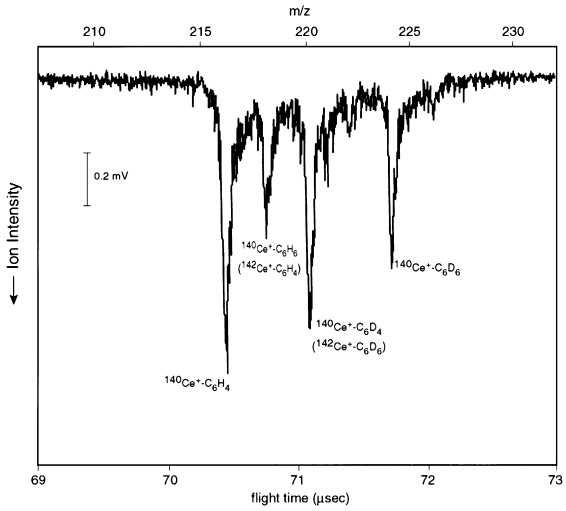

Fig. 4. Mass spectrum of products of the reaction of Ce^+ (from $CeSi_2$) with a mixture of approximately equal partial pressures of C_6H_6 and C_6D_6. The concurrent intensity of bare Ce^+ was ~100 mV.

4. Conclusions

Experiments were carried out to illuminate the ablation of Ln^+ from discrepant compounds and to assess the nature of reactions of these Ln^+ with cyclic hydrocarbons. The main conclusions are summarized as follows:

(1) Ion ablation: discrepant ion yields from different compounds ablated under identical conditions indicates ionization close to the solid surface, probably involving electron transfer processes. Small polyatomics such as LnO^+ form prior to mixing in the ablation plume, perhaps by direct ejection from the solid.

(2) Role of Ln^{+}* in dehydrogenation: discrepant reactivities were determined for the same Ln^+ ablated from different solids. This is interpreted to indicate a role for excited-state Ln^{+}* chemistry and counsels discretion in designing and interpreting Ln^+ reaction studies.

(3) Isotope effects in Ln^+-hydrocarbon collisions: product distributions from deuterated benzenes reflected relatively enhanced proton loss, consistent with the KIE. Loss of H_2 and D_2 from benzene-1,3,5-d_3 may reflect hydrogen scrambling and/or elimination of non-adjacent hydrogens.

LAMB is a relatively simple and versatile approach to examining gas-phase chemistry, specifically f element organometallic chemistry. Compared with more sophisticated and complex techniques, such as FTICR-MS, the LAMB method is particularly well-suited to applications under constrained circumstances such as imposed by highly radioactive materials. In this regard, the laser ablation mass spectrometer has recently been integrated into an α-containment glovebox, and gas-phase organometallic chemistry studies of transuranic actinides have been initiated.

Acknowledgements

This work was sponsored by the Division of Chemical Sciences, Office of Basic Energy Sciences, US Department of Energy, under Contract DE-AC05-96OR22464 at Oak Ridge National Laboratory with Lockheed Martin Energy Research Corp.

References

[1] J.K. Gibson, J. Phys. Chem. 100 (1996) 15688–15694.
[2] J.K. Gibson, Anal. Chem. 69 (1997) 111–117.
[3] H.H. Cornehl, C. Heinemann, D. Schroder, H. Schwarz, Organometallics 14 (1995) 992–999.
[4] L.S. Sunderlin, P.B. Armentrout, J. Am. Chem. Soc. 111 (1989) 3845–3855.
[5] J.H. El-Nakat, I.G. Dance, K.J. Fisher, G.D. Willett, Polyhedron 12 (1993) 2477–2487.
[6] E.R. Fisher, R.H. Schultz, P.B. Armentrout, J. Phys. Chem. 93 (1989) 7382–7387.
[7] K. Sugiyama, J. Yoda, Phys. Rev. A 55 (1997) R10–R13.

[8] H. Higashide, T. Oka, K. Kasatani, H. Shinohara, H. Sato, Chem. Phys. Lett. 163 (1989) 485–489.
[9] J.K. Gibson, J. Phys Chem. 98 (1994) 6063–6067; J.K. Gibson, J. Phys. Chem. 98 (1994) 11321–11330.
[10] J.K. Gibson, J. Fluorine Chem. 78 (1996) 65–74.
[11] Miller, J. C., Laser Ablation—Principles and Applications, Springer-Verlag, New York, 1994.
[12] I.H. Musselman, R.W. Linton, D.S. Simons, Anal. Chem. 60 (1988) 110–114.
[13] L.A. Bloomfield, Y.A. Yang, P. Xia, Z. Phys. D 20 (1991) 461–463.
[14] J.K. Gibson, J. Appl. Phys. 78 (1995) 1274–1280; J.K. Gibson, J. Phys. Chem. 100 (1996) 507–511.
[15] J.K. Gibson, J. Vac. Sci. Technol. A 13 (1995) 1945–1958.
[16] H. Hotop, W.C. Lineberger, J. Phys. Chem. Ref. Data 14 (1985) 731–750.
[17] K.B. Blagoev, V.A. Komarovskii, Atomic Data Nuclear Data Tables 56 (1994) 1–40.
[18] S.K. Loh, E.R. Fisher, L. Lian, R.H. Schultz, P.B. Armentrout, J. Phys. Chem. 93 (1989) 3159–3167.
[19] W.W. Yin, A.G. Marshall, J. Marcalo, A. Pires de Matos, J. Am. Chem. Soc. 116 (1994) 8666–8672.
[20] R. Marquardt, W. Sander, E. Kraka, Angew. Chem. Int. Ed. Engl. 35 (1996) 746–748.
[21] P.G. Wenthold, J.A. Paulino, R.R. Squires, J. Am. Chem. Soc. 113 (1991) 7414–7415.
[22] P.G. Wenthold, J. Hu, R.R. Squires, J. Am. Chem. Soc. 118 (1996) 1865–1871.
[23] D. Stockigt, J. Hrusak, H. Schwarz, Int. J. Mass Spec. Ion Processes 149–150 (1995) 1–11.
[24] R.C. Dunbar, Int. J. Mass Spec. Ion Processes 100 (1990) 423–443.